Use of acute hyperphenylalaninemia in rhesus monkeys to examine sensitivity and stability of the L-[1-11C]leucine method for measurement of regional rates of cerebral protein synthesis with PET

Carolyn B Smith[1], Kathleen C Schmidt[1], Shrinivas Bishu[1], Michael A Channing[2], Jeff Bacon[2], Thomas V Burlin[1], Mei Qin[1], Zhong-hua Liu[1], Zengyan Xia[1], Tianjiang Huang[1], Bee-Kee Vuong[2] and Peter Herscovitch[2]

[1]Section on Neuroadaptation and Protein Metabolism, National Institute of Mental Health, Bethesda, Maryland, USA; [2]PET Department, Clinical Center, National Institutes of Health, Bethesda, Maryland, USA

We have previously shown by direct comparison with autoradiographic and biochemical measurements that the L-[1-11C]leucine positron emission tomography method provides accurate determinations of regional rates of cerebral protein synthesis (rCPS) and the fraction (λ) of unlabeled leucine in the precursor pool for protein synthesis derived from arterial plasma. In this study, we examine sensitivity of the method to detect changes in λ and stability of the method to measure rCPS in the face of these changes. We studied four isoflurane-anesthetized monkeys dynamically scanned with the high resolution research tomograph under control and mild hyperphenylalaninemic conditions. Hyperphenylalaninemia was produced by an infusion of phenylalanine that increased plasma phenylalanine concentrations three- to five-fold. In phenylalanine-infused monkeys, plasma leucine concentrations remained relatively constant, but values of λ were statistically significantly decreased by 11% to 15%; rCPS was unaffected. Effects on λ are consistent with competitive inhibition of leucine transport by increased plasma phenylalanine. The effect on λ shows that competition for the transporter results in a reduction in the fraction of leucine in the precursor pool for protein synthesis coming from plasma. Even under these hyperphenylalaninemic conditions, rCPS remains unchanged due to the compensating increased contribution of leucine from protein degradation to the precursor pool.

Introduction

The L-[1-11C]leucine positron emission tomography (PET) method for the determination of regional rates

of cerebral protein synthesis (rCPS) is an adaptation of the quantitative autoradiographic L-[1-14C]leucine method (Smith *et al*, 1988) developed for use in experimental animals. The theoretical basis and validity of the method were described previously (Schmidt *et al*, 2005; Smith *et al*, 2005). The PET method requires dynamic scanning to estimate the model parameters that are then used to calculate the fraction (λ) of the precursor leucine pool for protein synthesis derived from arterial plasma. This critical aspect of the method provides a means to quantify (1-λ) the relative contribution of leucine recycled from tissue proteolysis to the precursor pool in the tissue; recycled leucine is unlabeled and will dilute the precursor pool specific activity. If recycling is not taken into account, rCPS measurements will be in error. By comparison of the results of parallel PET and L-[3,4,5-3H(N)]leucine studies in adult

rhesus monkeys, we showed the validity of the compartmental modeling approach for the estimation of λ (Smith *et al*, 2005).

The present study was undertaken to test the sensitivity of the L-[1-11C]leucine PET method to detect changes in the value of λ. In a genetic mouse model of phenylketonuria (PKU) in which arterial plasma phenylalanine concentration was 20 times normal, we had shown previously that the value of λ determined by a direct biochemical method is decreased by 37% (Smith and Kang, 2000). In this study, in adult monkeys, we administered an intravenous infusion of phenylalanine designed to increase and maintain plasma phenylalanine concentrations three to five times normal levels. Under conditions of both hyperphenylalaninemia and normal levels of plasma amino acids in the same animals, we applied the L-[1-11C]leucine PET method, evaluated the parameters of the method and λ, and determined rCPS in whole brain and regions of gray and white matter. We found that even with fairly mild hyperphenylalaninemia, the L-[1-11C]leucine PET method has the sensitivity to detect 11% to 15% decreases in the values of λ, but that rCPS is unaffected.

Materials and methods

Kinetic Model

The model for the behavior of leucine in brain (Figure 1) includes four rate constants: K_1 and k_2 for carrier-mediated transport from plasma to brain and back from brain to plasma, respectively; k_3 for metabolism of leucine to yield CO_2; and k_4 for incorporation of leucine into protein. The rate constants are identical for the labeled and unlabeled species, except that we have included a rate constant for breakdown of unlabeled tissue protein, k_5, in the model; we assume that there is no significant breakdown of the labeled protein during the experimental interval. Unlabeled leucine is assumed to be in a steady state.

The total concentration of 11C in the field of view of the PET camera (C_T^*) at time T is comprised of free [11C]leucine and [11C]protein in the tissue (C_E^* and P^*, respectively), diffusible 11CO$_2$ in the tissue (C_D^*), products of 11CO$_2$ fixation (C_F^*), and activity in the blood in the brain ($V_b C_b^*$), where V_b is the fraction of the volume occupied by blood and C_b^* is the measured total activity in whole blood. It is assumed that 11CO$_2$ in brain is rapidly equilibrated with the arterial blood (Buxton *et al*, 1987), so that $C_D^* \approx V_D C_a^*$, where C_a^* is the measured 11CO$_2$ activity in whole blood and V_D is the brain/blood equilibrium distribution volume of 11CO$_2$ ($V_D = 0.41$; Smith *et al*, 2005). We also assumed negligible fixation of 11CO$_2$ during the experimental period (Buxton *et al*, 1987; Siesjö and Thompson, 1965), that is, $C_F^* \approx 0$. Therefore,

$$C_T^*(t) \approx (1 - V_b)\left[C_E^*(t) + P^*(t) + V_D C_a^*(t)\right] + V_b C_b^*(t) \quad (1)$$

In the course of a study, labeled leucine in the tissue is derived solely from the arterial plasma. Unlabeled leucine, however, is derived from both the arterial plasma
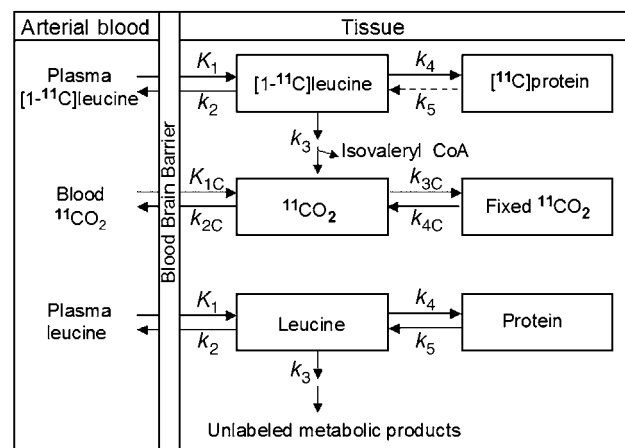
Figure 1 Compartmental model of leucine in brain. The exchangeable pool in brain (either labeled or unlabeled) includes intracellular, extracellular, and tRNA-bound leucine. K_1 and k_2 are the rate constants for carrier-mediated transport of leucine from plasma to tissue and from tissue to plasma, respectively. k_3 is the rate constant for the first two steps in the catabolism of leucine, which includes a transamination reaction followed by a rapid decarboxylation. The rate constant for leucine incorporation into protein is represented by k_4, and that for release of free leucine by protein degradation is k_5. Unlabeled leucine is assumed to be in a steady state. Owing to the long half-life of proteins in brain, it is assumed there is no significant loss of label from the radioactive protein within the experimental period, i.e., k_5 [(11C)protein] = 0. After an injection of leucine labeled on the carboxyl carbon, the only possible labeled metabolites in brain are α-ketoisocaproic acid (α-KIC), CO_2, and products of CO_2 fixation. As there is very little labeled α-KIC in brain (Keen *et al*, 1989), this pool is not explicitly represented in the model and k_3 combines the transamination and decarboxylation reactions, as noted above. Labeled CO_2 can arise either through catabolism of labeled leucine in brain or through influx from the blood after the breakdown of labeled leucine in other tissues; once in the brain it may be either transported from brain to blood or fixed in brain. Pools of labeled CO_2 in the arterial blood and brain and labeled products of CO_2 fixation in the tissue are also represented in the model. K_{1C} and k_{2C} are the rate constants for influx and efflux of labeled CO_2 between brain and blood, respectively, and k_{3C} and k_{4C} represent the rate constants for fixation and loss of fixed CO_2, respectively.

and the steady-state breakdown of protein in the tissue. The fraction (λ) of unlabeled leucine in the precursor pool derived from arterial plasma is defined as

$$\lambda = \frac{\text{Influx from arterial plasma}}{[\text{Influx from arterial plasma} + \text{Flux from protein degradation}]} \quad (2)$$

Substituting from the kinetic model

$$\lambda = \frac{K_1 C_p}{[K_1 C_p + k_5 P]} \quad (3)$$

where C_p is the steady-state concentration of unlabeled leucine in arterial plasma and P is the concentration of unlabeled protein in the tissue. The influx of leucine from arterial plasma ($K_1 C_p$) not only depends on C_p but also on the plasma concentrations of large neutral amino acids

competing with leucine for the transporter at the blood–brain barrier. From Michaelis–Menten kinetics for competitive inhibition at the transporter,

$$K_1 C_p = \frac{V_{\max(leu)} C_p}{k_{m(leu)}\left[1 + \sum_{i=1(i \neq leu)}^{n} \frac{LNAA_{(i)}}{k_{m(i)}}\right] + C_p} + k_{D(leu)} C_p \quad (4)$$

where $V_{\max(leu)}$ is the maximal transport rate of the saturable transport component for leucine, $k_{m(leu)}$ is the half-saturation constant of the saturable component for leucine, $LNAA_{(i)}$ is the arterial plasma concentration of the ith large neutral amino acid that competes with leucine for the transporter (i = methionine, valine, isoleucine, tyrosine, and phenylalanine), $k_{m(i)}$ is the corresponding half-saturation constant for the amino acid, and $k_{D(leu)}$ is the rate constant for nonsaturable transport of leucine across the blood–brain barrier. Equation (4) can be rearranged to

$$K_1 C_p = \frac{V_{\max(leu)} C_p}{k_{m(leu)}\left[1 + \sum_{j=1}^{n} \frac{LNAA_{(j)}}{k_{m(j)}}\right]} + k_{D(leu)} C_p \quad (5)$$

where the sum is now comprised of all the large neutral amino acids that share the carrier, including leucine (j = methionine, valine, isoleucine, leucine, tyrosine, and phenylalanine). If we define S as the denominator in equation (5), that is, as the sum of concentrations of the large neutral amino acids that share the carrier, weighted by their respective half-saturation constants and by $k_{m(leu)}$, that is,

$$S = k_{m(leu)}\left[1 + \sum_{j=1}^{n} \frac{LNAA_{(j)}}{k_{m(j)}}\right] \quad (6)$$

then equation (5) can be rewritten as

$$K_1 C_p = V_{\max(leu)}\left[\frac{C_p}{S}\right] + k_{D(leu)} C_p \quad (7)$$

Dividing both sides of equation (7) by C_p yields

$$K_1 = V_{\max(leu)}\left[\frac{1}{S}\right] + k_{D(leu)} \quad (8)$$

Equation (8) defines the relationship between the weighted sum of the large neutral amino acids that share the L-amino-acid transporter and the influx rate constant for leucine, K_1. K_1 decreases as the concentrations of the large neutral amino acids in the plasma increase.

The effect of large neutral amino-acid concentrations on influx relates to their effect on λ (see equation (3)). Recall that unlabeled leucine is in steady state; hence the rates of protein synthesis and degradation are equal, that is,

$$k_5 P = k_4 C_E = rCPS \quad (9)$$

where C_E is the concentration of free leucine in the tissue. Substituting equations (7 and 9) into equation (3) yields

$$\lambda = \frac{V_{\max(leu)}\left[\frac{C_p}{S}\right] + k_{D(leu)} C_p}{V_{\max(leu)}\left[\frac{C_p}{S}\right] + k_{D(leu)} C_p + rCPS} \quad (10)$$

Equation (10) explicitly describes the effects that leucine and the weighted sum of the large neutral amino acids

have on λ. As C_p approaches 0, $\lambda \to 0$, that is, the only source of unlabeled leucine in the precursor pool for protein synthesis is from protein breakdown. As C_p increases, the weighted sum of all the amino acids (including leucine) necessarily also increases, and $\lambda \to 1$, that is, the unlabeled leucine in the precursor pool derived from protein breakdown is negligible, compared with that derived from the arterial plasma. Equation (10) also predicts that an increase in S, with no change in C_p or rCPS, will result in a decrease in λ. In this study, equation (10) was not used to predict the value of λ as estimates of the parameters $V_{\max(leu)}$, $k_{D(leu)}$, and rCPS that are independent of the present data were not available, but rather the equation was used to predict the direction of the change in λ that would result from the changes in plasma amino acids.

Animals

All procedures were performed in accordance with the National Institutes of Health Guidelines on the Care and Use of Animals and an animal study protocol approved by the Clinical Center Animal Care and Use Committee. We studied four adult male rhesus monkeys (10 to 15 kg). Surgical preparation of the animals under isoflurane anesthesia took place at least 4 weeks before the study and consisted of inserting a polyurethane catheter attached to a Port-A-Cath vascular port (Sims Deltec Inc., St Paul, MN, USA) into a femoral artery and securing the port under the skin of the ipsilateral thigh. Catheters were flushed weekly with heparinized saline to maintain patency. Each animal was studied two to three times under control and once under hyperphenylalaninemic conditions.

Magnetic Resonance Imaging

Magnetic resonance images (MRI) used to identify regions of interest (ROIs) on the PET images were obtained from each of the monkeys while under ketamine anesthesia. Animals were positioned in an MRI-compatible stereotactic head holder. Two animals were scanned with a General Electric Signa 1.5 T scanner (GE Medical Systems, Milwaukee, WI, USA) with a 5-inch GP surface coil. A T1-weighted three-dimensional (3D) gradient echo sequence with RF spoiling (TR (repetition time)/TE (echo time)/flip angle, 25/6 ms/30°) was used with a field of view of 10 cm and slice thickness of 1 mm. Two animals were scanned with a 4.7-T vertical Bruker magnet (Bruker BioSpin Corp., Billerica, MA, USA). A T1-weighted 3D MDEFT (modified-driven equilibrium Fourier transform) was used with 0.5 mm³ isotropic voxel size.

Preparation of L-[1-^{11}C]Leucine

D,L-[1-^{11}C]Leucine was prepared from H^{11}CN with a modified Strecker–Bucherer reaction sequence (Studenov et al, 2003). The isolation of the pure L-amino acid isomer from the racemic mixture was achieved by chiral HPLC (high-performance liquid chromatography) with a

Chirobiotic T column (10×250 mm) (Advanced Separation Technologies Inc., Whippany, NJ, USA), mobile phase of ethanol/water: 5:95 (v/v), and a flow rate of 3 mL/min. Retention times of the L- and D-isomers were approximately 7 and 8 mins as determined by the corresponding standards. The L-[1-^{11}C]leucine was obtained with a radiochemical purity of >99% and an estimated specific activity of 108 GBq/μmol at the end of bombardment.

Phenylalanine Infusion

To achieve hyperphenylalaninemia, animals were administered intravenously a programmed infusion of 1.5% (w/v) phenylalanine in normal saline. The infusion was initiated 60 mins before the scheduled L-[1-^{11}C]leucine injection and maintained throughout the length of the PET study. The infusion program was designed to achieve and maintain a constant and elevated phenylalanine concentration in arterial plasma and was calculated based on the clearance curve of an intravenous pulse injection of phenylalanine (Patlak and Pettigrew, 1976).

PET Studies

Before each PET study, animals were fasted overnight. In the morning, the animals were sedated with ketamine and intubated, and intravenous lines were inserted into both legs. The head was immobilized in a stereotactic head holder, and the animal was positioned in the PET scanner face forward so that scanning was in a coronal plane. The sedated animal was then anesthetized and studied under isoflurane anesthesia. Isoflurane was maintained at a mean alveolar concentration of 1.0% to 1.1%. Studies were performed with an ECAT High Resolution Research Tomograph (HRRT) (CPS Innovations, Knoxville, TN, USA). Each leucine study was preceded by a 6-min transmission scan to correct for attenuation and three 60-sec H$_2$^{15}O (0.15 GBq per scan) scans 15 mins apart to aid in registering PET and MR images. Leucine studies were initiated by the intravenous infusion of L-[1-^{11}C]leucine (0.18 to 0.36 GBq) over 1 min. Dynamic PET acquisition began at the time of injection. Scans were obtained in list mode and reconstructed with a 3D ordinary Poisson OSEM algorithm (Carson *et al*, 2003) as 30 frames of data (8×15 secs, 4×30 secs, 6×60 secs, 4×150 secs, 8×300 secs). All activities were decay-corrected to the time of injection of the radiopharmaceutical. The reconstructed volume consisted of 207 slices of the head, 1.22 mm in thickness. Spatial resolution was $\sim$2.5 mm full width at half maximum (FWHM) in the transverse and axial direction in the center of the field of view (Wienhard *et al*, 2002); the field of view was 31.2 cm (transverse plane) by 25.2 cm (axial plane).

Analysis of Blood Samples

Arterial blood samples were collected every 4 to 10 secs for the first 2 mins and at increasing intervals thereafter to measure the time courses of total ^{11}C and ^{11}CO$_2$ activity in arterial blood and the concentrations of leucine and [^{11}C]leucine in plasma over the 60 mins scan duration. Blood samples were apportioned for the various determinations as follows: (1) Approximately 0.2 to 0.3 mL of blood was transferred to a tube containing 1 N NaOH; the tube was weighed and counted in a gamma counter (Cobra II Auto Gamma, Packard Instrument Co. Inc., Downers Grove, IL, USA) to obtain total activity in whole blood. (2) Approximately 0.5 mL was centrifuged to remove red cells, and 0.2 mL of plasma from each sample was diluted in distilled water and deproteinized at 4°C by the addition of a solution of 16% (w/v) sulfosalicylic acid containing L-norleucine (0.04 mM) as an internal standard for amino-acid analysis. Concentrations of labeled leucine in the acid-soluble fractions were assayed by gamma counting, and concentrations of unlabeled leucine and other large neutral amino acids, that is, methionine, valine, isoleucine, tyrosine, and phenylalanine, were assayed by fluorescence detection of postcolumn *O*-phthaldehyde derivatized amino acids separated with ion exchange HPLC (Agilent Technologies Inc., Santa Clara, CA, USA and Pickering Laboratories Equipment, Mountain View, CA, USA). (3) Approximately 1 mL of whole blood was injected through the septum of a sealed vial into 2 mL of 8% sulfosalacylic acid. Attached to the septum of the vial was a polyethylene cup with a filter paper soaked with 1 N NaOH. The vial was weighed, and after allowing 30 mins for the evolution of ^{11}CO$_2$, the filter paper was removed and counted.

Positron Emission Tomography Data Analysis

Three-dimensional volumes were constructed for the average of the three [^{15}O]water scans and for each frame of the [^{11}C]leucine scan. The reconstructed [^{15}O]water volume was aligned to the MRI volume by the use of the Automated Image Registration program with a 3D rigid body transformation (Woods *et al*, 1993); the transformation parameters were subsequently applied to each frame of the [^{11}C]leucine scan to effect its alignment to the MRI volume. Regions of interest were drawn on the MRIs and transferred to the [^{11}C]leucine volumes to compute tissue time activity curves (TACs). We analyzed the brain as a whole, cerebellum, somatosensory cortex, striate cortex, putamen, and corona radiata; and in the four animals studied, volumes (mean ± s.d.) were 100.7 ± 16.3, 10.1 ± 3.5, 0.8 ± 0.2, 4.3 ± 1.2, 1.2 ± 0.5, 2.2 ± 2.0 mL, respectively. For each ROI, the rate constants K_1, $k_2 + k_3$, and k_4, and V_b were estimated by a weighted nonlinear least squares fit of the model to the measured blood curves and tissue TACs (equation (1)) (Schmidt *et al*, 2005). Assuming Poisson statistics, weights were inversely proportional to the s.d. of the decay-corrected activity in each frame of data as follows:

$$\text{s.d.}(C_T(t_i)) = N\sqrt{e^{\gamma t_i} C_T(t_i)/\Delta t_i} \qquad (11)$$

where γ is the decay constant for ^{11}C, t_i the midpoint of Frame *i*, and Δt_i the length of Frame *i*. (Under Poisson

statistics, the s.d. in the number of counts (x_i) in each frame of data equals $\sqrt{x_i}$. Therefore, before decay correction, the mean count rate in each frame of data ($y_i = x_i/\Delta t_i$) has s.d. $\sqrt{y_i/\Delta t_i}$, and the s.d. for the decay-corrected mean count rate ($C_T(t_i) = e^{\gamma t_i} y_i$) is given by $\sqrt{e^{\gamma t_i} C_T(t_i)/\Delta t_i}$. In equation (11) N is a proportionality coefficient that encompasses other noise effects that are constant in a given region throughout the study; any additional noise effects were not included in the weights. The difference between the tracer arrival time in the brain and the arterial sampling site was estimated by shifting the blood TAC 0 to 10 secs, fitting the whole brain TAC, and selecting the delay time that produced the best fit of the data. Since in human studies, differences in tracer appearance time in various parts of the brain differ from the brain as a whole by not more than ± 2 secs (Iida *et al*, 1988), the whole brain value was used for all regions in our studies. Label in CO_2 fixation products in the tissue was assumed to be negligible. λ was then calculated from the ratio of rate constants (Schmidt *et al*, 2005) as follows:

$$\lambda = \frac{k_2 + k_3}{k_2 + k_3 + k_4} \quad (12)$$

rCPS was computed from the mean arterial plasma leucine concentration, C_p (nmol/mL), and the fitted values for the rate constants (and λ) for each ROI as

$$\text{rCPS} = \frac{K_1 k_4}{k_2 + k_3} C_p = \left(\frac{K_1 k_4}{k_2 + k_3 + k_4} \right) \frac{C_p}{\lambda} \quad (13)$$

For each study, S, the sum of the amino acids that share the large neutral amino-acid carrier (methionine, valine, isoleucine, leucine, tyrosine, and phenylalanine), weighted by their respective half-saturation constants, k_m, was computed by equation (6). As k_m has not been measured in the monkey, values determined in the adult rat were used (Smith *et al*, 1987). The least squares best fitting straight line between estimates of K_1 and $1/S$ (see equation (8)) were determined for all regions and whole brain.

Statistical Analyses

Paired comparisons were made between the mean of baseline studies in each monkey and its phenylalanine-infused study. Differences in mean values of time-weighted average LNAA concentrations during the 60 min PET study, regional values of λ, and rCPS were analyzed for statistical significance by means of two-tailed paired *t*-tests. An *F*-test was used to assess whether the slope of the best fitting line between K_1 and $1/S$ was different from zero.

Results

After initiation of the programmed infusion of L-phenylalanine, arterial plasma phenylalanine concentrations were increased by about 10 times control values, and within 60 mins leveled off at about 3 to 5 times baseline (Figure 2A). Concentrations remained fairly constant (coefficient of variation (COV) 4% to 13%) for the following 60 min period (0 to 60 mins on the abscissa, Figure 2A) during which time the L-[1-¹¹C]leucine PET study was conducted. Most large neutral amino-acid concentrations in plasma were unaffected by the phenylalanine infusion except tyrosine which was increased by 80% to 160% (Figures 2A and 2B). Most importantly, arterial plasma leucine concentrations were similar under both conditions (Figure 2B) and remained relatively constant over the course of the 60 min PET study (Figure 2A) (COV of 1% to 3%). During the PET study, most physiologic variables measured were similar under both control and hyperphenylalaninemic conditions (Table 1). Only body weight and mean arterial blood pressure were statistically significantly different. Animals were on average 4% heavier at the time of the phenylalanine infusion study and mean arterial blood pressure was on average 11% lower during the phenylalanine infusion studies.
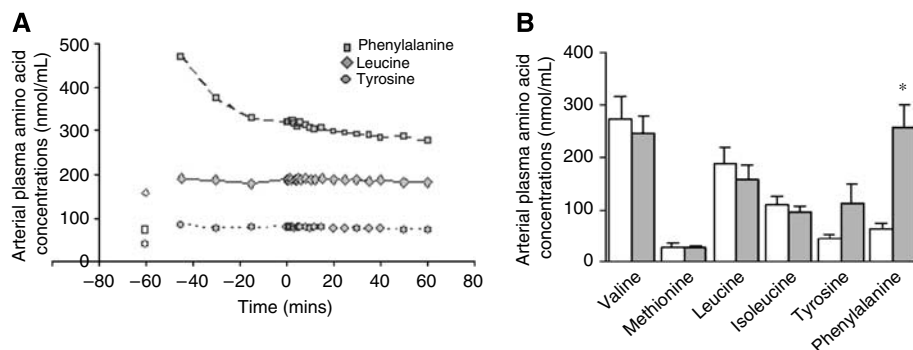
Figure 2 Arterial plasma concentrations of large neutral amino acids. (**A**) Time course of concentrations of phenylalanine, leucine and tyrosine after the commencement of an intravenous programmed infusion of phenylalanine in a typical study. The open symbols represent baseline amino-acid concentrations and filled symbols concentrations after the initiation of the phenylalanine infusion at −60 mins. The [¹¹C]leucine PET study began at 0 time. (**B**) Time-weighted average amino-acid concentrations during the [¹¹C]leucine PET study. Bars represent the means ± s.d. of the means of baseline studies in four monkeys (open bars) and four phenylalanine-infused (filled bars) studies. Differences between the two conditions were assessed by paired *t*-tests; *Statistically significantly different, $P < 0.01$.

Table 1 Physiological variables at the time of the PET study

	Baseline (4)	PHE infused (4)[a]
Body weight (kg)	12.6 ± 1.9	13.1 ± 1.9*
Body temperature (°C)	36.7 ± 0.1	36.5 ± 0.7
Respiration rate (breaths per min)	23 ± 3	23 ± 5
Heart rate (beats per min)	110 ± 10	111 ± 15
Mean arterial blood pressure (mm Hg)	76 ± 7	67 ± 3*
Arterial blood pH	7.40 ± 0.02	7.40 ± 0.04
Arterial blood pCO_2 (mm Hg)	43.8 ± 2.1	44.3 ± 2.1
Arterial blood pO_2 (mm Hg)	371 ± 30	424 ± 114
Arterial plasma glucose concentration (mg%)	72 ± 7	75 ± 6

PET, positron emission tomography; PHE, phenylalanine.
Values are the means ± s.d. for the number of animals indicated in parentheses. Animals were studied two to three times under baseline conditions, and values are the means ± s.d. of the means from each of the four animals.
*Statistically significantly different from baseline mean, $P < 0.05$; paired Student's t-tests.
[a]$N = 3$ for measurements of pH, pCO_2, and pO_2 in PHE-infused group.

Typical clearance curves for total ^{11}C activity in whole blood, $^{11}CO_2$ in whole blood, and free [^{11}C]leucine in arterial plasma in a baseline and phenylalanine infusion study are shown in Figures 3A and 3B, respectively. Except for the first few minutes, curves were similar under both conditions. In this particular pair of studies, activity in the blood increased earlier in the phenylalanine-infused animal compared with the baseline study (Figure 3C). Across all studies, we found that the lag between the start of the [^{11}C]leucine infusion and the appearance of activity in the arterial blood varied between 14 and 29 secs. This variability is probably due to slight differences in the mechanics of injection among the studies. In these two studies, differences in the blood activity during the first 2 mins are reflected in the very early parts of the measured time courses of total activity in visual cortex (Figure 3F). Full measured time courses of total activity for primary visual cortex in the same studies are shown in Figures 3D and 3E, respectively. Also shown in Figures 3D and 3E are the model-predicted time courses of ^{11}C activity in the tissue distributed among the blood, free leucine, CO_2, and protein pools. Despite the higher activity in blood in the hyperphenylalaninemic animal (Figure 3B compared with 3A), the total activity in visual cortex is lower (Figure 3E) compared with the baseline study (Figure 3D). The model-predicted activity in the free leucine pool increases steadily and at a similar rate in the first 5 mins under both conditions, but in the hyperphenylalaninemic animal, it peaks at a lower level and as it clears remains below the level in the baseline study. Under both baseline and hyperphenylalaninemic conditions, predicted activity in the protein compartment increases progressively so that by 60 mins it comprises 83% and 84% of the activity, respectively. In whole brain, predicted activity in the free leucine compartment in control and hyperphenylalaninemic animals increases for the first 5 mins to an average of 73% and 71% of the total activity, respectively, and progressively decreases thereafter to 12% and 9% of the total at 60 mins, respectively; predicted activity in the protein compartment is an average of 79% and 84%, respectively, at 60 mins. Under both conditions, most (50% to 90%) of the predicted activity is in blood during the first 1.5 mins, but by 10 mins blood accounts for about 7% of the total and by 60 mins 3%. Predicted activity in CO_2 increases to 4% of the total by 5 mins and remains fairly constant thereafter in both control and phenylalanine-infused animals.

The estimated rate constants and blood volumes in whole brain and five ROIs are shown in Table 2. The half-life of leucine in the tissues ($\ln(2)/[k_2 + k_3 + k_4]$) was between 4 and 6 mins under both conditions. Consistent with a partial saturation of the transporter by the elevated plasma phenylalanine concentration, estimates of K_1, the influx rate constant from plasma to brain, were lower in the hyperphenylalaninemic animals, ranging from 18% lower in primary visual cortex to 27% lower in putamen. Effects were statistically significant in whole brain and in four of the five regions examined. We found a linear relationship between estimates of K_1 and $1/S$ (Figure 4) in whole brain and in all regions examined. Slopes were positive and statistically significantly different from zero ($P < 0.05$) in all regions and whole brain.

Estimates for the sum ($k_2 + k_3$) of the rate constants for efflux from the brain to plasma and for metabolism of leucine in the brain had a tendency to be lower in the phenylalanine-infused animals, whereas estimates for the rate constant for leucine incorporation into protein, k_4, tended to be higher in hyperphenylalaninemic animals (Table 2). We found statistically significant linear relationships between estimates of $k_2 + k_3$ and $1/S$ in whole brain and in somatosensory cortex and putamen; the r^2 for the linear relationship between $k_2 + k_3$ and $1/S$ was 0.3257 ($P = 0.03$), 0.3552 ($P = 0.02$), and 0.3093 ($P = 0.04$) in whole brain, somatosensory cortex, and putamen, respectively. There were no statistically significant linear relationships between estimates of k_4 and $1/S$ in whole brain or any of the regions. Estimates of V_b tended to be slightly lower in the phenylalanine-infused animals, but these differences were not statistically significant (Table 2). In controls, mean estimates of λ ranged from 0.70 to 0.78 in whole brain and regions, whereas in hyperphenylalaninemic animals, estimates of λ were 11% to 15% lower, ranging from 0.60 to 0.68 (Figure 5A).

Computed rCPS were similar in both groups of animals (Figure 5B). Average rates (± s.d.) for baseline studies ranged from 2.01 ± 0.58 in corona radiata to 3.18 ± 0.14 nmol/g/min in primary visual cortex. Regional rate of cerebral protein synthesis in
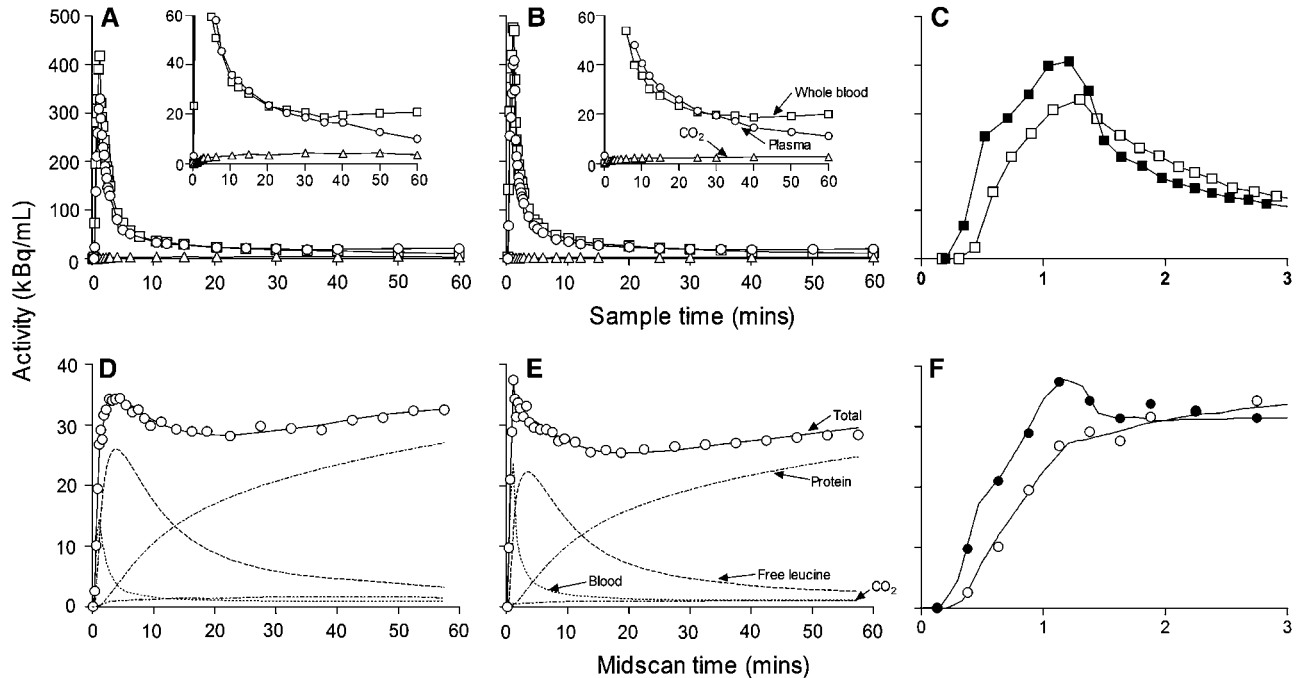
Figure 3 Arterial clearance curves from a typical baseline (**A**) and phenylalanine infusion (**B**) study in the same monkey and the respective time courses of ^{11}C activity in primary visual cortex after intravenous injection over 1 min of 0.36 GBq L-[1-^{11}C]leucine ((**D**) baseline and (**E**) phenylalanine infusion). For both the baseline and phenylalanine infusion studies, the first 3 mins of activity in whole blood (**C**) and of total activity measured and estimated in visual cortex (**F**) are also shown. In panels A and B, open squares (□) represent the total ^{11}C activity in whole blood, open circles (○) the activity of free [^{11}C]leucine in plasma, and the open triangle (△) the activity in $^{11}CO_2$ in whole blood. The insets in panels A and B are the figures with the scale on the ordinate expanded. In panel **C**, the open (□) and filled (■) squares represent the total activity in whole blood in baseline and phenylalanine infusion studies, respectively, and the solid lines connect the sampled points. In panels D and E, open circles (○) represent the total activity measured at each time point in the ROI. In each figure, the solid line is the total activity predicted by the model. The dashed and dotted lines are the activities predicted by the model in the pools in the tissue as labeled on the figure: free leucine, protein, CO_2, and blood in the brain. In panel F, the open (○) and filled (●) circles represent the total activity measured in the ROI in baseline and phenylalanine infusion studies, respectively, and the solid lines represent the total activity predicted by the model for each study. Parameter estimates in primary visual cortex in this baseline study (**C**) were $K_1 = 0.052$ mL/g/min; $(k_2 + k_3) = 0.137$ min^{-1}; $k_4 = 0.053$ min^{-1}; $V_b = 0.044$, tracer delay = 6 secs. Parameter estimates in primary visual cortex in this phenylalanine infusion study (**D**) were $K_1 = 0.045$ mL/g/min; $(k_2 + k_3) = 0.149$ min^{-1}; $k_4 = 0.059$ min^{-1}; $V_b = 0.058$, tracer delay = 3 secs.

white matter was about 40% of the rate in cortical grey matter. Coefficients of variation for the four animals were 2% to 11% in grey matter regions and 29% in corona radiata.

Parameteric images of rCPS from one of the studies are shown in Figure 6. Differences in rCPS between grey and white matter areas are clear, and the heterogeneity of rCPS within cortex and in subcortical grey matter is apparent. In extracerebral structures, there is a clear incorporation of leucine into protein in scalp muscle and salivary glands.

Discussion

Our results show both the sensitivity and robustness of the L-[1-^{11}C]leucine PET method. In response to increases in the plasma concentrations of phenylalanine, estimates of K_1 and calculated values of λ were decreased. The effect on λ shows that competition for the blood–brain barrier transporter results in a reduction in the fraction of leucine in the

precursor pool for protein synthesis coming from plasma. Even under these hyperphenylalaninemic conditions, rCPS remained unaffected likely due to the compensating increased contribution of leucine from protein degradation to the precursor pool $(1-\lambda)$.

The L-[1-^{11}C]leucine PET method (Schmidt *et al*, 2005) is the first fully quantitative method for the measurement of rCPS with PET. The method is fully quantitative because it takes into account recycling of unlabeled leucine derived from tissue protein breakdown into the precursor pool for protein synthesis. Effects of leucine recycling are accounted for by λ calculated as a ratio of parameters (equation (12)) estimated from a fit of the model to measured blood and tissue TACs. The validity of this approach was established by comparison of PET results with biochemical determinations (Smith *et al*, 2005). From the equation for rCPS (equation (13)), it is clear that an error in the value of λ will result in an inversely proportional error on calculated rCPS. Even relatively small errors in rCPS are problematic because effects of different conditions and disease

Table 2 Regional estimates of parameters of the leucine model

Region	K_1 (mL/g/min)		k_2+k_3 (min^{-1})		k_4 (min^{-1})		V_b	
	Baseline (4)	PHE infused (4)	Baseline (4)	PHE infused (4)	Baseline (4)	PHE infused (4)	Baseline (4)	PHE infused (4)
Whole brain	0.039±0.004	0.030±0.004*	0.116±0.009	0.092±0.013*	0.045±0.005	0.055±0.004**	0.044±0.003	0.042±0.009
Cerebellum	0.037±0.002	0.027±0.004*	0.127±0.019	0.099±0.018*	0.052±0.005	0.064±0.004**	0.053±0.002	0.051±0.009
Somatosensory cortex	0.037±0.002	0.028±0.004*	0.097±0.010	0.070±0.010*	0.042±0.007	0.047±0.001	0.041±0.004	0.037±0.009
Primary visual cortex	0.047±0.009	0.038±0.005	0.136±0.024	0.118±0.022	0.050±0.007	0.063±0.006*	0.043±0.005	0.043±0.011
Putamen	0.046±0.005	0.033±0.005*	0.116±0.008	0.088±0.019	0.032±0.002	0.041±0.002*	0.039±0.004	0.033±0.004
Corona radiata	0.027±0.003	0.020±0.002*	0.108±0.008	0.081±0.012*	0.043±0.005	0.051±0.012	0.026±0.003	0.025±0.006

PHE, phenylalanine; V_b, fraction of brain volume occupied by blood.
Statistically significantly different from control value, paired t-test; *$P < 0.05$, **$P < 0.01$.
Values are the means ± s.d. for the number of animals indicated in parentheses. Animals were studied two to three times under baseline conditions and values reported are the means ± s.d. of the means for each of the four animals.

states on rCPS are not expected to be large. On the basis of our experience in rodent experiments with the L-[1-^{14}C]leucine autoradiographic method, most effects on rCPS are <20% (Smith, 1991; Qin *et al*, 2005).

Estimates of K_1 and λ and measurements of rCPS in this series of animals studied under baseline conditions agree well with results reported previously in a different series of monkeys (Smith *et al*, 2005). In whole brain, estimates of λ and rCPS were within 0.1% and 5% of previously reported values, respectively. In all five regions examined, values of λ were almost identical and measured rCPS were within 8% of previously reported values. The agreement between the results of this study and our previous study in a different series of animals studied with a lower resolution camera attest to the reproducibility and stability of the measurements.

In this study, we have examined the sensitivity of the PET method to detect changes in the value of λ. The PET method requires dynamic scanning for 60 mins to estimate the parameters. In these initial studies, we have been careful to measure (rather than fit or estimate from population averages) any variable that can be directly measured. For example, in each study, we have measured the time courses in arterial blood of total ^{11}C, ^{11}CO$_2$, and [^{11}C]leucine and unlabeled leucine in plasma over the entire course of the study. We used a 60-min scanning interval having determined previously that rCPS values measured at 60 mins were in very good agreement with rates determined with the autoradiographic L-[1-^{14}C]leucine method (Smith *et al*, 2005). In this study, we made four changes to the procedure used previously (Smith *et al*, 2005). First, we used the HRRT scanner with a higher spatial resolution (FWHM of ∼2.5 mm) than the GE Advance PET Scanner (FWHM of 4.9 mm) used in our previous study. Second, we used a nonlinear fitting routine, having found that there is some bias in the linear fitting method (KC Schmidt, unpublished data). Third, we included the ^{11}CO$_2$ tissue compartment, having developed a more reliable method to quantify the ^{11}CO$_2$ concentration in the blood. Fourth, we have corrected the TACs of blood samples for the best fitting value of the delay of tracer arrival between the arterial sampling site and the brain.
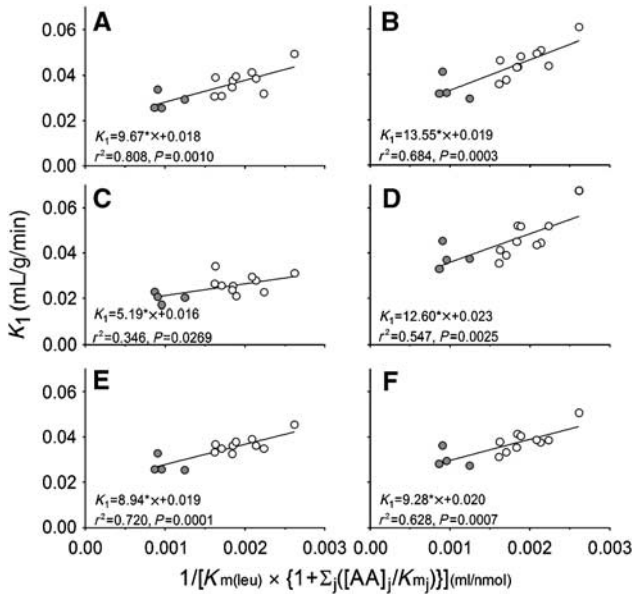
We are encouraged by the low variability of our estimates of λ and the relatively low variability of our determinations of rCPS. In whole brain and the five regions examined, COVs of λ estimates ranged from 3% to 5% in the 10 control studies and from 4% to 9% in the four phenylalanine infusion studies. Coefficients of variation of rCPS measurements in all 14 studies ranged from 11% in primary visual cortex to 25% in the corona radiata. The COV for the measurement of rCPS in whole brain was 11%. Knowledge of the variance in rCPS measurements is critical for the design of future studies and the consideration of the number of subjects required to detect changes of <20%.

The effects of hyperphenylalaninemia on estimates of K_1 for an amino acid competing for the

L-amino-acid transporter at the blood–brain barrier reported here are in good agreement with literature results. In [¹¹C]aminocyclohexanecarboxylate PET studies in healthy human volunteers, estimates of K_1 were decreased by about 50% when plasma phenyl-

Figure 4 The linear relationship between estimates of K_1 and

$$\left(k_{m\,(leu)} \left[1 + \sum_{j=1}^{n} \frac{LNAA_{(j)}}{k_{m(j)}} \right] \right)^{-1}$$

in all studies both controls (open symbols) and phenylalanine infused (filled symbols) in (**A**) secondary somatosensory cortex, (**B**) putamen, (**C**) corona radiata, (**D**) primary visual cortex, (**E**) cerebellum, and (**F**) whole brain. For each region, the least squares best fitting line was determined. For each graph, the best fitting equation, r^2 and the P-value are given. The slope of the line is an estimate of V_{max} for leucine transport across the blood–brain barrier and the Y-intercept is an estimate of k_D, the rate constant for nonsaturable transport of leucine.

alanine concentrations were increased by approximately 10-fold (Shulkin et al, 1995). As in our [¹¹C] leucine study, the rate constant for efflux of [¹¹C] aminocyclohexanecarboxylate was less affected. Similarly in an application of the double indicator method to a study of patients with PKU, permeability surface area product (PS) for leucine was reduced by about 50% compared with controls (Knudsen et al, 1995). In a study of [¹¹C]methionine uptake in phenylketonuric children on and off a low phenylalanine diet, Comar et al (1981) showed that phenylalanine levels in plasma increased on average about 10-fold and [¹¹C]methionine uptake decreased by about 50% while blood methionine concentration was unaffected. All of these studies show the partial saturation of the L-amino-acid transporter by the elevated plasma phenylalanine and the consequent inhibition of the uptake for competing amino acids.

The sensitivity of the [¹¹C]leucine method to detect these expected effects on one (K_1) of the four estimated parameters was not known. The linear relationship between estimates of K_1 and the reciprocal of the Michaelis–Menten expression for competitive inhibition further describes the behavior of the saturable carrier under these conditions. From the slopes of the lines, we can estimate V_{max} for transport of leucine into the brain in monkey under these experimental conditions. In primary visual cortex, V_{max} is estimated to be 13 nmol/g/min and the intercept, k_D, 0.02 mL/g/min. These estimates are within the range of values for V_{max} and k_D reported for the adult rat (Smith et al, 1987).

We had also predicted that under hyperphenylalaninemic conditions, the value of λ would be decreased. This prediction was based on the partial saturation of the transporter by elevated plasma phenylalanine concentrations coupled with normal leucine concentrations. Phenylalanine has the highest affinity for the transporter with a k_m of 0.011 μmol/mL; the k_m for leucine is 0.029 μmol/mL
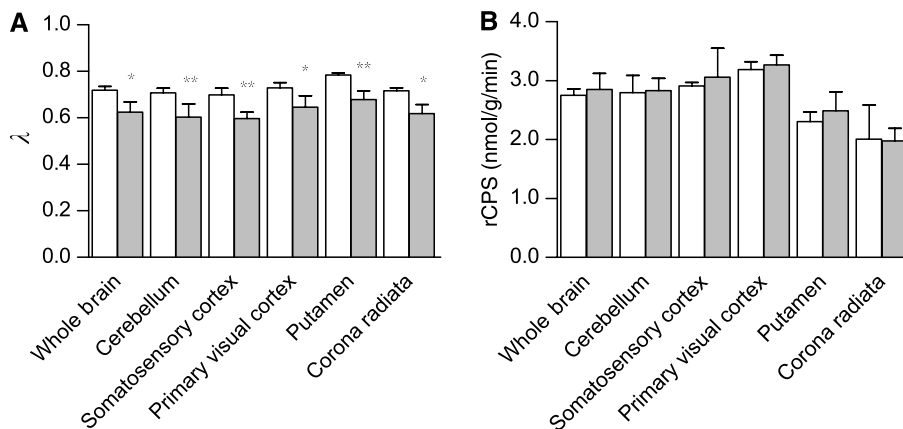
Figure 5 Effects of phenylalanine infusion on values of (**A**) λ and (**B**) rCPS in five regions of interest and whole brain. Bars represent means ± s.d. of the means of baseline studies in four monkeys (open bars) and the phenylalanine-infused (filled bars) studies in the same animals. In each region, means were compared by paired t-tests. Values of λ were statistically significantly lower in all regions in phenylalanine-infused animals; *$P < 0.05$; **$P < 0.001$.
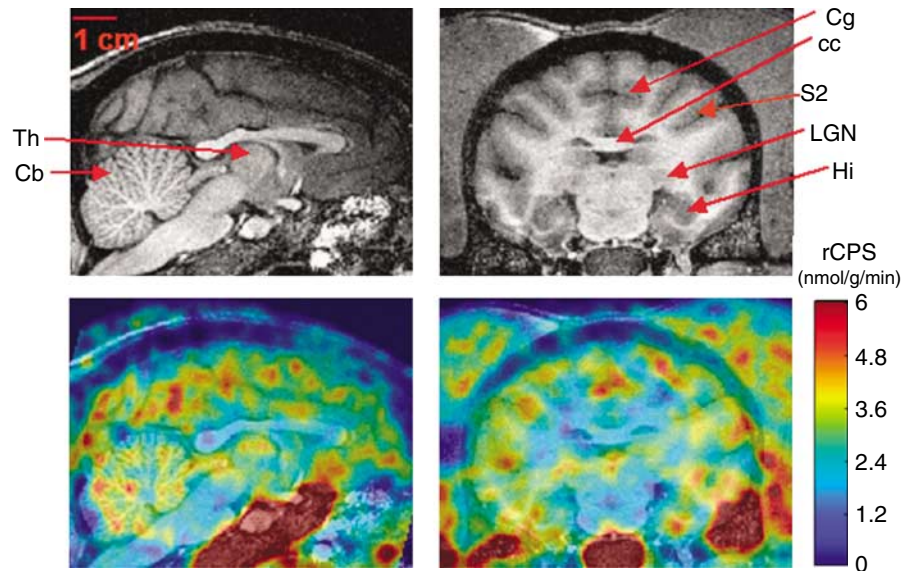
Figure 6 L-[1-11C]leucine PET images from studies in rhesus monkeys. Magnetic resonance images (upper panel) correspond to the [11C]leucine PET images (lower panel). Sagittal view at the midline is shown on the left, and coronal view at the level of the hippocampus is shown on the right. [11C]Leucine PET images are color-coded for rCPS; color bar is to the right of the first PET image. Slice thickness is 0.5 mm. Regional rate of cerebral protein synthesis was computed from the total activity in each voxel in each 5-min frame of data between 45 and 60 mins by use of an alternate equation for rCPS (equation (3) in Smith et al, 2005) and whole brain rate constants and λ estimated from the dynamic PET study of this animal, i.e., $K_1 = 0.040$ mL/g/min, $k_2 + k_3 = 0.111$ min^{-1}, $k_4 = 0.046$ min^{-1}, $\lambda = 0.71$, $V_b = 0.049$, $V_D = 0.41$. Regional rate of cerebral protein synthesis shown is the average of rCPS in the three frames of data. Bar in the upper left MR image is 1 cm and applies to all four images. Abbreviations: Th, thalamus; Cb, cerebellum; Cg, cingulate gyrus; cc, corpus callosum; S2, secondary somatosensory cortex; LGN, lateral geniculate nucleus; Hi, hippocampus.

(Smith et al, 1987). Normally, the transporter is saturated about equally with phenylalanine (37%) and leucine (36%). With a three- to five-fold elevation in plasma phenylalanine concentration, the transporter is 70% saturated with phenylalanine and 15% saturated with leucine. With this limitation in transport of leucine, we predicted a decrease in the ratio in equation (3). Our data show that the L-[1-11C]leucine method has the sensitivity to detect these effects.

In spite of the effect of hyperphenylalaninemia on λ, rCPS remained unchanged in our monkeys. This result agrees with the results in adult rats in which plasma phenylalanine concentrations were acutely elevated about 10-fold with no effects on rCPS (Dunlop et al, 1994). It is in neonatal animals that hyperphenylalaninemia appears to affect brain protein synthesis. Hyperphenylalaninemia resulted in a disaggregation of brain polyribosomes (Aoki and Siegel, 1970), an increase in 80S monoribosomes (Taub and Johnson, 1975), and a decrease in Met-tRNA$_i^{met}$ (Hughes and Johnson, 1977) in neonatal mice. The decreased concentration of Met-tRNA$_i^{met}$ suggested a decreased rate of initiation of brain protein synthesis possibly through a decrease in the initiation complex (Taub and Johnson, 1975). In accord with the results in neonatal mice and in contrast with the findings of this study, our studies of a genetic mouse model of PKU showed 20% decreases in rCPS throughout the brain in untreated adult mice (Smith and Kang, 2000). There are two important differences between our previous study on the adult mouse PKU model and this study. First, in this study, phenylalanine concentrations were increased three- to five-fold, whereas in our study of the PKU mouse model, plasma phenylalanine concentrations were about 21 times normal. There may be a critical concentration of plasma phenylalanine where brain protein synthesis is affected in the adult. Second, there may be a difference between the effects of acute and chronic hyperphenylalaninemia. In the mouse study, animals were hyperphenylalaninemic for their entire lives even during brain development. In this study, hyperphenylalaninemia was induced 1 h before the initiation of the PET measurement of rCPS. Further, the brains of adult mice with genetic PKU were smaller than controls (Smith and Kang, 2000), suggesting that the period of hyperphenylalaninemia during brain development may have caused deficiencies in brain structure. Decreased rCPS in adult mice with genetic PKU may reflect developmental structural abnormalities.

Our data not only show the sensitivity of the L-[1-11C]leucine PET method to detect effects of mild hyperphenylalaninemia on estimates of parameters but also the robustness of the method to these changes. In addition, our data show the necessity of estimating parameters in each study to obtain accurate and reproducible measures of rCPS.

1398

Disclosures

The authors state no duality of interest.

References

Aoki F, Siegel FL (1970) Hyperphenylaninemia: disaggregation of brain polyribosomes in young rats. *Science* 168:129–30

Buxton RB, Alpert NM, Babikian V, Weise S, Correia JA, Ackerman RH (1987) Evaluation of the ¹¹CO₂ positron emission tomographic method for measuring brain pH. I. pH changes measured in states of altered pCO₂. *J Cereb Blood Flow Metab* 7:709–19

Carson RE, Barker WC, Liow J-S, Johnson CA (2003) Design of a motion-compensation OSEM list-mode algorithm for resolution-recovery reconstruction for the HRRT. *IEEE Nucl Sci Symp Conf Rec* 5:3281–5

Comar D, Saudubray JM, Duthilleul A, Delforge J, Maziere M, Berger G, Charpentier C, Todd-Pokropck A, Crouzel M, Depondt E (1981) Brain uptake of ¹¹C-methionine in phenylketonuria. *Eur J Pediatr* 136:13–9

Dunlop DS, Yang X-R, Lajtha A (1994) The effect of elevated plasma phenylalanine levels on protein synthesis rates in adult rat brain. *Biochem J* 302:601–10

Hughes JV, Johnson TC (1977) The effects of hyperphenyl-alaninemia on the concentrations of aminoacyl-transfer ribonucleic acid *in vivo*. *Biochem J* 162:527–37

Iida H, Higano S, Tomura N, Shishido F, Kanno I, Miura S, Murkami M, Takahashi K, Sasaki H, Uemura K (1988) Evaluation of regional differences of tracer appearance time in cerebral tissues using [¹⁵O]water and dynamic positron emission tomography. *J Cereb Blood Flow Metab* 8:285–8

Keen RE, Barrio JR, Huang S-C, Hawkins RA, Phelps ME (1989) *In vivo* cerebral protein synthesis rates with leucyl-transfer RNA used as a precursor pool: determination of biochemical parameters to structure tracer kinetic models for positron emission tomography. *J Cereb Blood Flow Metab* 9:425–45

Knudsen GM, Hasselbalch S, Toft PB, Christensen E, Paulson OB, Lou H (1995) Blood–brain barrier transport of amino acids in healthy controls and in patients with phenylketonuria. *J Inher Metab Dis* 18:653–64

Patlak CS, Pettigrew KD (1976) A method to obtain infusion schedules for prescribed blood concentration time courses. *J Appl Physiol* 40:458–63

Qin M, Kang J, Burlin T, Smith CB (2005) Post-adolescent changes in regional cerebral protein synthesis: an *in vivo* study in the *Fmr1* null mouse. *J Neurosci* 25:5087–5095

Schmidt KC, Cook M, Qin M, Kang J, Burlin T, Sokoloff L, Smith CB (2005) Measurement of regional rates of cerebral protein synthesis with L-[1-¹¹C]leucine and PET with correction for recycling of tissue amino acids: I. Kinetic modeling approach. *J Cereb Blood Flow Metab* 25:617–28

Shulkin BL, Betz AL, Koeppe RA, Agranoff BW (1995) Inhibition of neutral amino acid transport across the human blood–brain barrier by phenylalanine. *J Neurochem* 64:1252–7

Siesjö BK, Thompson W (1965) The uptake of inspired ¹⁴CO₂ into the acid-labile, the acid-soluble, the lipid, the protein and the nucleic acid fractions of rat brain tissue. *Acta Physiol Scand* 64:182–92

Smith CB (1991) The measurement of regional rates of cerebral protein synthesis *in vivo*. *Neurochem Res* 16:1037–45

Smith CB, Schmidt K, Bacon J, Bishu S, Burlin T, Channing M, Huang T, Liu Z, Qin M, Vuong B, Xia Z, Herscovitch P (2007*b*) PET measurement of regional rates of cerebral protein synthesis with L-[1-¹¹C]leucine in adult monkeys: effects of large neutral amino acid concentrations on parameter estimates. *J Nucl Med* 48(Suppl 2):238P

Smith CB, Deibler GE, Eng N, Schmidt K, Sokoloff L (1988) Measurement of local cerebral protein synthesis *in vivo*: influence of recycling of amino acids derived from protein degradation. *Proc Natl Acad Sci USA* 85: 9341–9345

Smith CB, Kang J (2000) Cerebral protein synthesis in a genetic mouse model of phenylketonuria. *Proc Natl Acad Sci USA* 97:11014–9

Smith CB, Schmidt KC, Bacon J, Bishu S, Burlin T, Channing M, Herscovitch P, Huang T, Liu Z-H, Qin M, Vuong B-K, Xia Z (2007*a*) Effects of hyperphenylalani-nemia on PET measurement of regional rates of cerebral protein synthesis with correction for recycling in adult monkeys. *J Cereb Blood Flow Metab* 27(Suppl 1) (XXIII-1): P02-5U

Smith CB, Schmidt KC, Qin M, Burlin T, Cook M, Kang J, Saunders R, Bacher J, Carson RE, Channing M, Eckelman WC, Herscovitch P, Laverman P, Vuong B-K (2005) Measurement of regional rates of cerebral protein synthesis with L-[1-¹¹C]leucine and PET with correction for recycling of tissue amino acids: II. Validation in rhesus monkeys. *J Cerebr Blood Flow Metab* 25: 629–640

Smith QR, Momma S, Aoyagi M, Rapoport SI (1987) Kinetics of neutral amino acid transport across the blood–brain barrier. *J Neurochem* 49:1651–8

Studenov AR, Szalda DE, Ding YS (2003) Synthesis of no-carrier added C-11 labeled D- and L-enantiomers of phenylalanine and tyrosine for comparative PET studies. *Nuc Med Biol* 30:39–44

Taub F, Johnson TC (1975) The mechanism of polyribo-some disaggregation in brain tissue by phenylalanine. *Biochem J* 151:173–80

Wienhard K, Schmand M, Casey ME, Baker K, Bao J, Eriksson L, Jones WF, Knoess C, Lenox M, Lercher M, Luk P, Michel C, Reed JH, Richerzhagen N, Treffert J, Vollmar S, Young JW, Heiss WD, Nutt R (2002) The ECAT HRRT: performance and first clinical application of the new high resolution research tomograph. *IEEE Trans Nucl Sci* 49:104–10

Woods RP, Mazziotta JC, Cherry SR (1993) MRI-PET registration with automated algorithm. *J Comput Assist Tomogr* 17:536–46